THE JOURNAL OF PHYSICAL CHEMISTRY C

Article

pubs.acs.org/JPCC

Single-Molecule Charge Transport and Electrochemical Gating in Redox-Active Perylene Diimide Junctions

Seyyedamirhossein Hosseini,[†] Christopher Madden,[‡] Joshua Hihath,[*,§] Shaoyin Guo,[‡] Ling Zang,[*,∥] and Zhihai Li[*,†]

[†]Department of Chemistry, Ball State University, Muncie, Indiana 47306, United States

[‡]Biodesign Institute, Arizona State University, Tempe, Arizona 85287, United States

[§]Department of Electrical and Computer Engineering, University of California, Davis, California 95616, United States

[∥]Department of Materials Science and Engineering, University of Utah, Salt Lake City, Utah 84108, United States

Supporting Information

ABSTRACT: A series of redox-active perylene tetracarboxylic diimide (PTCDI) derivatives have been synthesized and studied by electrochemical cyclic voltammetry and electrochemical scanning tunnelling microscopy break junction techniques. These PTCDI molecules feature the substitution of pyrrolidine at the bay (1,7-) position of perylene and are named pyrrolidine-PTCDIs. These moieties exhibit a small bandgap (2.1 eV) compared with the "normal" (unsubstituted) PTCDI molecule (2.5 eV). Pyrrolidine-PTCDIs were functionalized with different anchoring groups (thiol, amine, pyridine) for building metal−molecule−metal (m−M−m) junctions. The single-molecule conductance values of pyrrolidine-PTCDIs have been determined by analyzing a large number of molecular (m−M−m) junctions created between an STM tip and substrate using a statistical method. Furthermore, we studied the gate dependence of the single-molecule conductance by trapping a molecule between the two electrodes and recording the current as a function of electrochemical gate potential. The experimentally determined conductance values for these bay-substituted pyrrolidine-PTCDI molecules are about twice as much as the unsubstituted PTCDI molecules. The present work shows that single-molecule conductance can be tuned by the bandgap of a molecular system without significantly altering the conductance pathway.

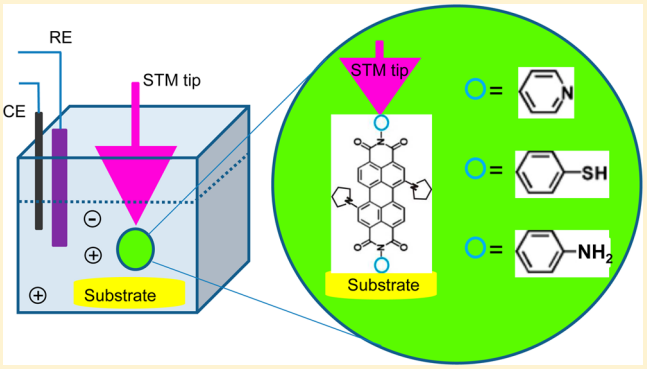

1. INTRODUCTION

Building an electronic device using individual molecules is one of the ultimate goals in nanotechnology.[1−7] As a key step toward molecular devices and future molecular electronics, measuring and controlling the electron transport through individual molecules attached to two electrodes have been investigated intensively.[6,8−19] Recently, an interest has focused on studies of electron transport through deliberately designed and synthesized molecules, revealing many intriguing phenomena as well as electron transfer mechanisms predicted by theoretical calculation.[20−22] For example, by using long conjugated molecular wires, several groups have observed the theoretically predicted change in direct-current transport from tunnelling to hopping as a function of systematically controlled wire length.[22−27] It was also found that the conductance of single-molecule junctions can be substantially modified by molecular conformation using a series of custom-designed molecules, which have similar biphenyl structures but with different twist angles.[9,28] Studies further show that the molecule-junction conductance is also influenced by other factors, such as the molecular anchoring groups,[29−35] π-stacking,[36] solution pH,[37,38] electrochemical potential,[10,39−42] electrode materials,[43,44] quantum interfere,[13,45,46] mechanical stretching,[47,48] photoswitching,[49−51] etc. However, only one report, to the best of our knowledge, correlated the charge transport with the bandgap of a molecular system at a single-molecule level.[52] In that work, an ambipolar transport in single-molecule junctions was discovered.[52]

In this contribution, we present direct transport measurements of deliberately synthesized perylene tetracarboxylic diimide (PTCDI) derivatives bridged across two electrodes in an electrochemical environment. PTCDI and its derivatives are attractive for molecular electronics as they represent a model redox system.[14,53,54] Tao et al. determined the conductance of PTCDIs at single-molecule level using scanning tunnelling microscopy (STM) break junction techniques and detected large electrochemical gating effect.[53] The Wandlowski group has investigated electrochemical and charge transport proper-

Received: June 20, 2016
Revised: August 9, 2016
Published: September 23, 2016

ACS Publications © 2016 American Chemical Society

DOI: 10.1021/acs.jpcc.6b06229
J. Phys. Chem. C 2016, 120, 22646−22654

ties of symmetrical and unsymmetrical PTCDI derivatives using spectro-electrochemical and electrochemical STM break junction techniques.[14,55] Though the concept of electrochemical (electrolyte) gating effect on the charge transport in molecules was initiated by White, Wrighton, and co-workers,[56] electrolyte gating of single organic molecule was experimentally achieved by Haiss et al.[10] and by Tao,[53] and further developed by other groups using STM and/or STM break junction techniques.[14,41,57−59] In an electrochemical electrolyte solution, charge transport can be regulated by external perturbation (electrode potential), so-called electrochemical gating.[10,20,39] In an STM break junction configuration, the potentials of STM tip and substrate electrodes, acting as the "source" and the "drain" electrodes, are independently controlled by a bipotentiostat using a reference electrode, i.e., the "gating electrode" (Figure 1A). Tuning the electrode potentials and energies of molecular orbitals, i.e., highest occupied molecular orbital (HOMO) and lowest unoccupied molecular orbital (LUMO), allows the Fermi level of electrodes to be aligned with these frontier molecular orbitals of the molecule in the junctions, thus to modulate the current through the junction.[20,21,41]

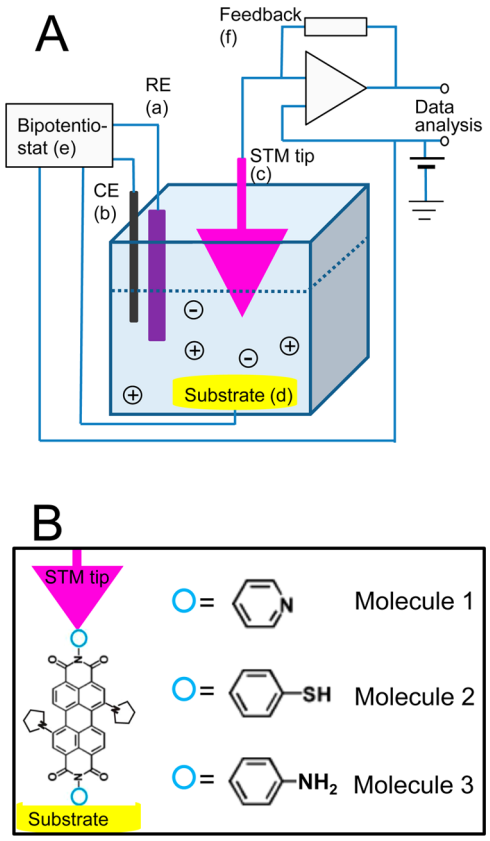

Figure 1. (A) Schematics of single-molecule conductance measurement in an electrochemical STM break junction configuration: (a) reference electrode (RE, also referred as gating electrode); (b) counter electrode (CE); (c) STM tip electrode; (d) substrate (sample) electrode; (e) bipotentiostat to control tip and substrate electrode potentials independently; (f) STM feedback system. (B) Pyrrolidine-PTCDI molecules bridged between two electrodes using different anchoring units in an electrochemical STM break junction. These molecules are labeled as molecule 1, molecule 2, and molecule 3, respectively, corresponding to PTCDIs having pyridinyl, thiophenyl, and aminephenyl as anchoring groups.

The target molecules in the present study are a series of perylene derivatives having a PTCDI backbone structure and two functional groups (pyrrolidinyl) substituted at the bay area. The structures of these pyrrolidinyl-substituted PTCDI are shown in Figure 1B. These PTCDI molecules exhibit smaller bandgap achieved by deliberately introducing two electron-donating dipyrrolidinyl groups at the 1,7 (bay)-positions, making the HOMO−LUMO gap for these bay-substituted PTCDIs as low as 2.1 eV (see UV−vis in Figure S4), in comparison with the normal PTCDI (2.5 eV).[52] The smaller band gap can facilitate the alignment of the Fermi level of electrodes to the HOMO and/or LUMO of the molecule in the junctions and give rise to the higher molecular conductivity. In this work, we also investigate their interfacial charge transport in three target molecules using cyclic voltammetry and study the electrochemical gating effect.

2. EXPERIMENTAL SECTION

2.1. Synthesis of Pyrrolidine-PTCDI Molecules. The pyrrolidine-PTCDIs were synthesized following the method reported before.[52] Briefly, 1,7-dipyrrolidinylperylene-3,4,9,10-tetracarboxylic acid dianhydride (0.2 mmol) and imidazole (4 g) were mixed with 4-aminopyridine, 4-aminothiophenol, or *p*-phenylenediamine (1.5 mmol each) and heated under argon at 100 °C for 3 h. After being cooled to room temperature, the mixture was dispersed into methanol (50 mL) followed by addition of dilute hydrochloric acid (1 M, 150 mL). The mixture was stirred for 12 h, and then the resultant green solid was collected by vacuum filtration. It was washed thoroughly with distilled water until the pH of washings became neutral. The collected solid was dried in vacuum and purified by column chromatography using CH_2Cl_2/CH_3OH as eluent.

2.2. Electrochemistry and Sample Preparation. Electrochemical measurements were performed in a three-electrode glass cell. A platinum wire serves as a counter electrode and a silver wire as a quasi-reference electrode for electrochemical experiments in $KClO_4$ electrolyte. We also carried out electrochemical cyclic voltammetry experiments in benzonitrile (BN) solution using 0.1 M tetrabutylammonium hexafluorophosphate ($TBAPF_6$) as the electrolyte and Ag/AgCl as a reference electrode. The working electrode is either a polycrystalline Au electrode (Bioanalytical Systems, 1.6 mm in diameter for cyclic voltammetry) or Au(111) film on mica (electrochemical STM break junction). The Au(111)/mica substrate was prepared by thermally evaporating gold on mica in a vacuum chamber, which provides a vacuum as low as 5×10^{-8} Torr. The thickness of the gold film on mica is 130 nm with typical terrace sizes around 100 nm × 100 nm. The electrodes were flame-annealed in a hydrogen flame and then cooled in high-purity argon atmosphere before experiments.

The thiolated pyrrolidine-PTCDI molecules (molecule 2) were assembled by immersing the substrate in 0.05 mM CCl_4 or THF solution overnight followed by copious rinsing with pure solvent to remove the extra layer of physisorbed molecules. Assembly of the amine (molecule 3) and pyridine (molecule 1) terminated pyrrolidine-PTCDIs were prepared by placing electrodes in a 1 mM CCl_4 solution for 2 min and then rinsed with pure solvent three times. The electrolyte solutions for the electrochemical STM experiments were prepared from Milli-Q water (18.2 M Ω) or ionic liquid. Benzonitrile containing $TBAPF_6$ (Fluka, electrochemical grade) as the electrolyte was used only for electrochemical cyclic voltammetry. All the electrolyte solutions were deaerated by bubbling in

DOI: 10.1021/acs.jpcc.6b06229
J. Phys. Chem. C 2016, 120, 22646−22654

an argon stream before and during experiments. For comparison we converted all potentials given in this article to a Ag/AgCl reference electrode.

2.3. Electrochemical STM Break Junction. The electrochemical STM break junction experiments were carried out with a Digital Instruments Nanoscope-E combined with a Molecular Imaging Bipotentiostat. The STM tips were fabricated by mechanically cutting a gold wire (0.25 mm diameter) or by electrochemically etching a gold wire in an electrolyte solution containing a mixture of 30% HCl and ethanol (1:1 in volume). The tips were coated with Apiezon wax to reduce leakage current, allowing control of the leakage current below 1 pA. The experimental procedure and data acquisition have been described previously.[8,21,58] The molecule-modified substrates were first imaged with a gold STM tip in a constant-current imaging mode. After we observed the surface terraces with clear and sharp atomic steps, which indicates a sharp tip and clean surface, the STM feedback loop was switched off. Meanwhile, a homemade LabVIEW program was activated to move the tip into and out of contact with the substrate at a rate of 20−40 nm/s. During this "tapping" process, molecules bridge across the two electrodes (STM tip and substrate) via the anchoring groups of molecules. The tapping process was automatically repeated for different preset bias values to generate a large number of conductance vs distance curves, typically 800−2000, for statistical analysis. Histograms in this study were constructed using all current−distance curves without selection.

As an example, Figure 2 illustrates how the single-molecule conductance was obtained by using a statistical analysis. The substrate potential was E_S = 0 V, and tip potential E_T = 0.1 V (Figure 2A blue) and 0.2 V (Figure 2A red), which gives rise to a bias voltage of 0.1 and 0.2 V. Typically the current decreases abruptly to a short conductance step/plateau before again decreasing to zero due to the large separation between the electrodes and the breakdown of a molecular junction. The current values of steps, corresponding to the current due to molecular conductance,[39,58] become doubled when bias voltages change from 0.1 to 0.2 V (Figure 2A). However, when current values were divided by the bias voltages applied, the resulting conductance values are very close or the same within error bars. Figure 2B shows two conductance histograms for molecule 1 measured at the different bias voltage of 0.1 and 0.2 V. Each histogram is constructed from 1015 and 850 individual conductance traces, respectively. The histograms measured at different bias voltages show peaks near 7×10^{-5} G_o, where $G_o = 2\ e^2/h \approx 77.4\ \mu S$. Figure S 1 shows the linear correlation between the junction current and bias voltage applied. From the slope of the linear fitting, it is confirmed that the single-molecule conductance value for molecule 1 is 7.1×10^{-5} G_o. We also performed tapping experiments using a tip and a bare substrate without adding target molecules as control experiments. The typical current traces in these control experiments are decay curves as shown in Figure S2, and no peak was observed in histograms constructed from these curves.

As an alternative approach, the conductance of the bay-substituted PTCDI molecules was also determined by performing molecular "blinking" experiments. In these experiments, instead of driving an STM tip into contact with a substrate covered with molecules and then retracting the tip to form molecular junction, we first imaged the molecule-modified surface, and then parked the tip at the center of a large terrace. After the system stabilized, the STM feedback was switched off and the tunnelling current was monitored. When a molecule bridges between the tip and the substrate, there is a jump in the current, which is attributed to the formation of a molecular junction. Once a stable molecular junction is formed, we swept the electrochemical gate potential (reference potential) and recorded the source−drain current as a function of gate voltage and time.

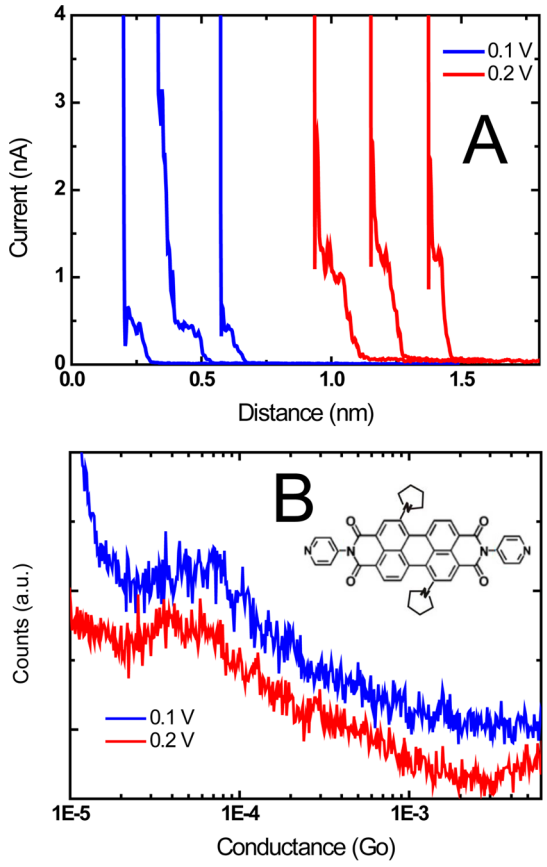

Figure 2. Single-molecule conductance of molecule 1—pyrrolidine-PTCDI terminated with pyridine anchoring groups. (A) Individual conductance traces, where the steps are due to the breakdown of the molecule−electrode contact. (B) Conductance histograms constructed from 1015 and 850 individual conductance traces measured at bias voltages of 0.1 and 0.2 V, respectively. Inset: the structure of molecule 1.

3. RESULTS AND DISCUSSION

Electrochemical Cyclic Voltammograms. Figure 3 show a typical cyclic voltammogram (CV) of the thiol-terminated pyrrolidine-PTCDI (molecule 2) adsorbed on gold electrode. Electrochemical electrolyte was 0.1 M $KClO_4$ adjusted to pH = 11 by addition of NaOH. Contact with the electrolyte was established at E = 0.0 V to keep absorbed molecules in the oxidation form, and then the electrode potential was scanned negatively up to −1.1 V and then back to the initial potential of 0.0 V. The CVs for all three pyrrolidine-PTCDI molecules in the aqueous solution show one pair of current peaks near −0.7 V, corresponding to a reversible redox reaction, which is consistent with reported electrochemical response for redox-active PTCDIs.[14] The cathodic and anodic current peaks for the phenylthiol-terminated PTCDI are relatively symmetrical (Figure 3). In the case of pyridine- (molecule 1) and phenylamine-terminated (molecule 3) PTCDIs, the cathodic

DOI: 10.1021/acs.jpcc.6b06229
J. Phys. Chem. C 2016, 120, 22646−22654

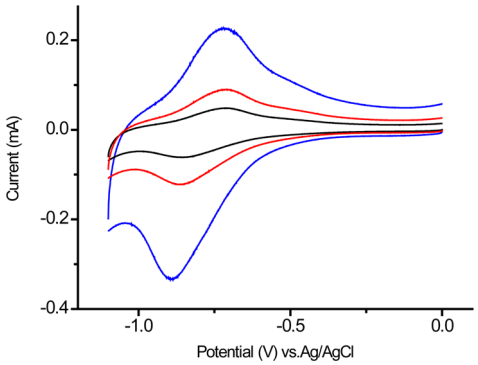

Figure 3. Cyclic voltammograms of a gold electrode modified with thiolated PTCDI (molecule 2) in a 0.1 $KClO_4$ solution, pH = 11 by addition of NaOH solution, at a scan rate of 0.1 V/s (black), 0.2 V/s (red), and 0.5 V/s (blue), respectively.

currents are apparently larger than the anodic currents (Figure S3). One possible reason for this could be that amine and pyridine group are physisorbed on the gold electrode, and the potential change could cause desorption or partial desorption of molecules from the electrode surface.[60] Therefore, the reduction process for these amine- and pyridine-terminated molecules could be overlapped with the partial desorption of molecules, which is not the case for thiol-terminated molecules.

The electrochemical cyclic voltammetry experiments were also carried out in an organic solvent. Figure 4 A, B, C illustrate

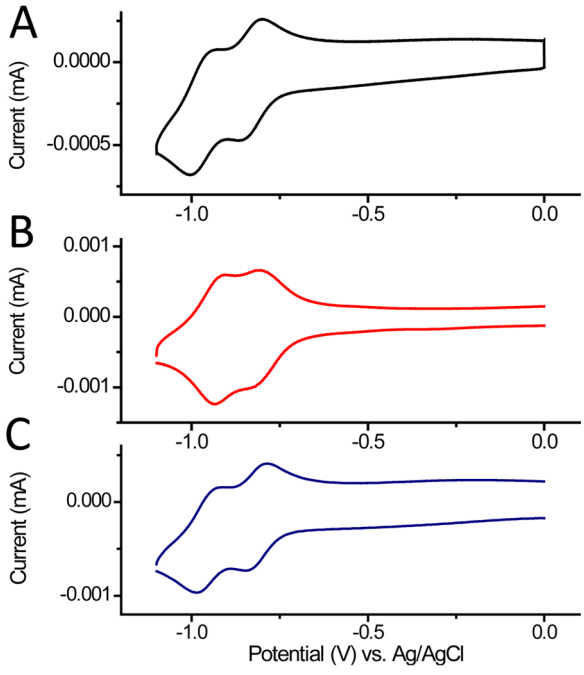

Figure 4. Cyclic voltammograms of a gold electrode modified with molecule 1 (A), molecule 2 (B), and molecule 3 (C), respectively, in benzonitrile solution containing 0.10 M tetrabutylammonium hexafluorophosphate ($TBAPF_6$).

the cyclic voltammograms of a gold electrode modified with pyrrolidine-PTCDIs terminated with pyridines (molecule 1), thiols (molecule 2), and amines (molecule 3) groups, respectively, in benzonitrile with $TBAPF_6$ as the supporting electrolyte. Compared with the CVs in the aqueous solution, two pairs of peaks can be readily identified from the CV in organic electrolyte (Figure 4). Two pairs of peaks in the CV of PTCDI derivatives adsorbed on gold electrode have been also reported in dichloromethane electrolyte and were attributed to the reversible reduction/oxidation processes of PTCDI/$PTCDI^-$and $PTCDI^-$/$PTCDI^{2-}$ species.[14]

The differences in the voltammetric behavior in organic solvents and an aqueous electrolyte are related to specific role of interfacial water and ion−molecule interactions. This assumption is supported by the fact that increasing the saturating level of water in organic solvent leads to a significantly smaller separation between the two current peaks.[14,41]

Molecular Junction Conductance. We carried out single-molecule conductance measurements of the three pyrrolidine-PTCDIs with different anchoring groups in both aqueous and ionic liquid solution. The latter medium provides wider potential windows for electrochemical gating measurements and gives smaller tip leakage/charging current than the aqueous solution. Therefore, we will focus our discussion on the electrochemical gating measurements in this medium. Figure 5 shows the typical individual conductance traces with current steps measured at 0.0 V gate potential. The corresponding histograms were constructed from 796, 797, 797 individual traces for molecule 1, molecule 2, and molecule 3, respectively. Interestingly, the peak of the conductance histogram is broader for molecules 1 and 3 (Figure 5B, D) than for molecule 2 (Figure 5C); this is likely due to the fact that the weaker binding to the electrodes with the amine or pyridine results in a larger variation of the measured conductance value. The histograms in Figure 5 show well-defined peaks near 7.1×10^{-5}, 3.5×10^{-5}, and 4.2×10^{-5} G_o for molecules 1, 2, and 3 respectively. The single-molecule conductance experiments were also performed in pH = 11, 0.1 M $KClO_4$ electrolyte for all three PTCDI molecules. Based on the same statistical analyses, the single-molecule conductance values in different electrolytes are shown in Table 1 for comparison. The conductance values are only slightly different for the same molecule in different electrolyte solutions, meaning that the electrolyte medium does not have a significant impact on the molecular conductance properties.[41] However, contact does have a significant effect on the molecular conductance as molecule 1 (pyridine-terminated PTCDI) has much larger conductance than molecules 2 (phenylthiol-terminated) and 3 (amine-terminated). The reason for these changes could be that molecule 1 has shorter coupling distance provided by the pyridine anchoring groups. It is also apparent that the conductance of molecule 2 is higher than molecule 3 which could be due to the relatively weak coupling of amine group with gold electrode compared with the strong thiol−gold coupling.[29,31]

Comparing our results with published data on the conductance of normal PTCDI molecules (without bay substitution) demonstrates the PTCDIs with the band gap reduced by the bay-substituted pyrrolidines show higher junction conductance than the normal PTCDI. For example, for the phenylthiol-terminated PTCDI with a normal bandgap of 2.5 eV, it has been reported that the single-junction conductance was 1.75×10^{-5} G_o.[61] In comparison, the present study reveals that the bay-substituted PTCDI (with a reduced bandgap, 2.1 eV) exhibits a conductance of 4.2×10^{-5} G_o, about 2.5 times higher than the regular PTCDI.[61] Similarly, the pyridine-terminated, bay-substituted PTCDI is 1.3 times higher than the equivalent "native" PTCDI at zero potential. However,

DOI: 10.1021/acs.jpcc.6b06229
J. Phys. Chem. C 2016, 120, 22646−22654

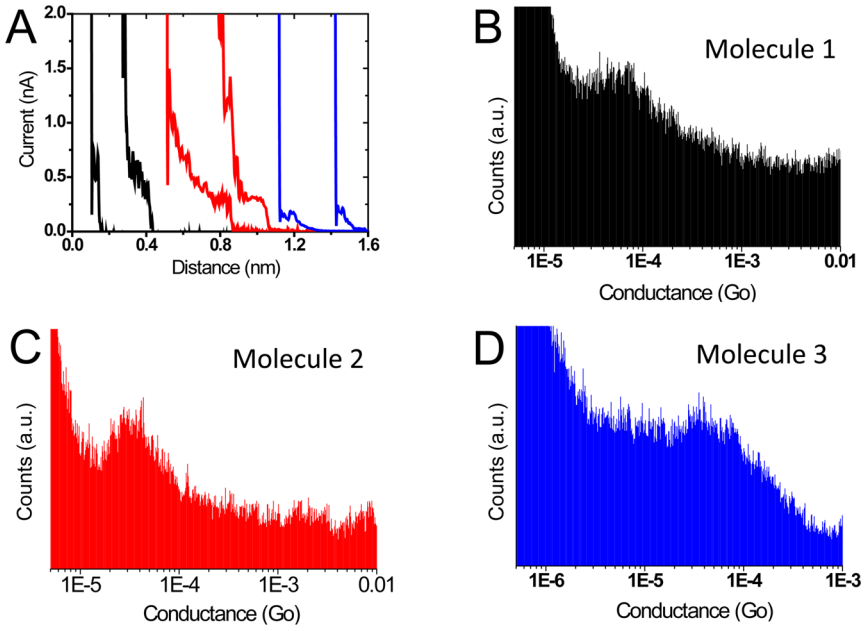

Figure 5. (A) Individual conductance traces of molecule 1 (black), molecule 2 (red), and molecule 3 (blue), E_{bias} = −0.1 V, E_{sample} = 0.0 V. (B−D) Conductance histograms constructed from 796, 797, and 797 individual conductance traces of molecules 1, 2, and 3, respectively.

Table 1. Conductance of Three Pyrrolidine-PTCDI Molecules in Ionic Liquid and pH = 11, 0.1 M $KClO_4$ Electrolytes

	conductance ($\times 10^{-5}$ G_o)		
electrolytes	molecule 1	molecule 2	molecule 3
ionic liquid	7.1 ± 2.1	4.2 ± 1.3	3.2 ± 1.4
0.1 M KClO4	7.8 ± 2.0	3.6 ± 0.9	2.6 ± 0.9

considering such a large change in bandgap (0.4 eV), the change in conductance seems smaller than expected. This observation indicates that in the present system it is the proximity of the electrode Fermi energy to the LUMO/HOMO energy level that dominates the conductance rather the HOMO−LUMO gap itself and suggests that the alignment between these energy levels is greatly affected by the specific linker group used. These results may stimulate theoretical investigation, for example, to reveal how the alignment of the LUMO/HOMO to the electrode Fermi energy can influence electron transport at a single-molecule level.

Electrochemical Gating. In an electrochemical STM setup, there are two working electrodes (the STM tip and substrate/sample electrode), a counter electrode, and a reference electrode, which is also referred to as a gate electrode. Both working electrodes are controlled by the reference electrode via a bipotentiostat (Figure 1).[10,20,61] Using the electrochemical STM break junction technique, we investigated the electrode gating effect of the three bay-substituted pyrrolidine-PTCDI molecules by the "tapping"[20] as well as the "blinking"[21] methods. For the tapping method, we recorded individual conductance traces at different preset gate potentials (sample potential) and constructed potential-dependent histograms to determine the gated conductance values. Figure 6 shows three conductance histograms of molecule 1 obtained at different gate potentials of 0.0, −0.3, and −0.5 V, respectively. By changing the gate potential negatively, one can clearly see the shifting of the pronounced conductance peaks in histograms to much higher conductance values.

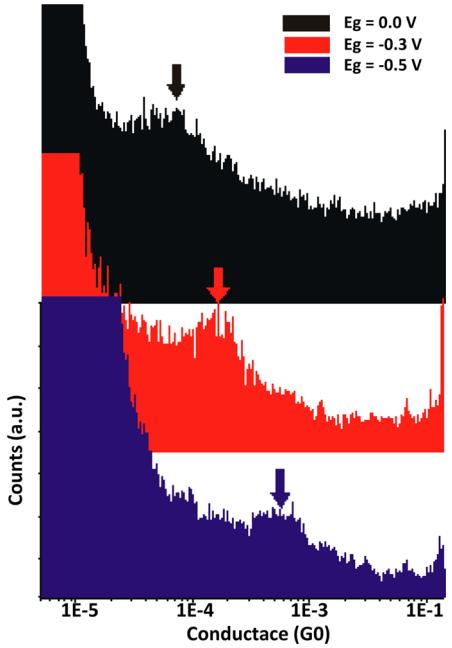

Figure 6. Conductance histograms of molecule 1 measured in an ionic liquid at 0.1 V bias and three different gate voltages (0.0, −0.3, −0.5 V). The three arrows indicate molecular conductance peaks and show that the conductance increases when gate potential was applied.

The electrochemical gate effects of the pyrrolidine-PTCDIs were also studied using blinking method. As described in the Experimental section, we positioned the STM tip close to molecules absorbed on the surface and monitored the tunneling current change. During the blinking process, we often observed that current abruptly jumped to higher value and then back to the original value, corresponding to the attachment/detachment of a PTCDI molecule to/from the STM tip through the linker group. A few typical blinking curves are shown for molecule 3 (Figure 7A, red curves) and molecule 2 (Figure 7B, blue curve) in an ionic liquid solution. In the case of molecule

DOI: 10.1021/acs.jpcc.6b06229
J. Phys. Chem. C 2016, 120, 22646−22654

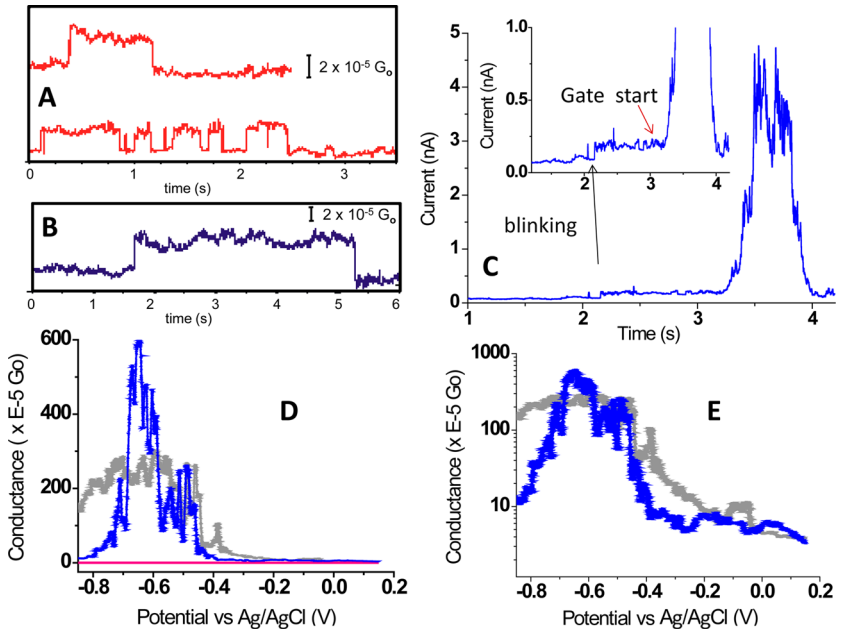

Figure 7. Electrochemical gate effect in pyrrolidine-PTCDI molecular junctions. (A, B) Conductance current vs time blinking events between the high- and low-current level, corresponding to the formation and breakdown of molecular junctions for molecules 3 (red) and 2 (blue), respectively. (C) Conductance current vs time curves for molecule 2. When the current switched to the high level as the inset shows, corresponding to the formation of a molecular junction between the tip and substrate electrode, sweeping the electrochemical gate potential causes a large change in the transport current. (D, E) Linear and logarithmic plotting of conductance vs gate potential for molecule 2 (blue) and molecule 3 (gray). The pink curve shows the leakage current of the tip with no molecular blinking during sweeping the gate potential.

3, it is evident that the current jumps to a higher value only for a short time, typically less than 1 s, and then switches back to the original value. Furthermore, we often observed multiple switching for this molecule (Figure 7A, the lower red curve), likely due to the weak coupling between the amine anchoring group and the gold tip. In case of molecule 2, the phenylthiol-terminated PTCDI, we frequently observed that the current switched to a higher value and lasted for a few seconds before it switched back to the original value. We attribute this observation to a stronger coupling between the thiol linker group and a gold tip. Such a stable junction allows us to run an electrochemical gate potential and simultaneously record the source-drain current as a function of time and gate voltage before the molecular junction broke down. Figure 7C shows a typical curve of the current vs time trace of a single PTCDI junction obtained while sweeping the gate potential. When we zoom in (the inset curve), one sees that the initial current is small and stable, and then at 2.1 s the current suddenly switches to a higher value, corresponding to the formation of a molecular junction between the tip and substrate. Dividing the current (0.15 nA) by the bias applied (0.05 V) gives rise to a conductance value of 3.9×10^{-5} G_o, which is consistent with the conductance value extracted from the histogram in Figure 5C. At ∼ 3 s, as indicated by the red arrow, we started to run the gate potential from 0.0 to −1.0 V and back to 0.0 V. One may see that after sweeping the gate potential, the current is almost the same as the original value, indicating that the molecular junction remained intact during the potential sweeping process.

To clearly see the gate effect, we also plotted a blinking and gate curve as conductance versus gate voltage. Figure 7 D and E show how the source-drain current change as a function of gate voltage. The molecular junction conductance increased gradually while the gate voltage swept negatively and reached a maximum, 2 orders of magnitude larger than the conductance at zero gate voltage. To elucidate the electrochemical current contribution from the tip electrode to the source-drain current measured above, we retracted the tip out of the tunneling regime and recorded the electrochemical current from the tip electrode as a function of gate voltage. As the pink curve in Figure 7D demonstrates, the leakage current from tip electrode is extremely small, typical 1−2 pA, which is negligible in comparison with the molecular junction current. Control experiments using a bare substrate and tip without adding target molecules yielded no clear blinking events, and no electrochemical gating was detected. The interpretation for the enhancement of molecular conductance is that by adjusting the gate voltage, one can shift the Fermi level of source and drain electrodes (STM tip and substrate) toward the HOMO or LUMO levels. When the Fermi level of source or drain electrode was approaching the HOMO or LUMO levels, the tunneling through the molecule was enhanced and reached a maximum when the Fermi level of one electrode was aligned to the HOMO or LUMO levels.[10]

These results provide new insights into the charge transport mechanism involved in these molecular systems. Since the redox state for this molecule is accessible via electrochemical gating, it is possible that either a two-step hopping mechanism or a LUMO-dominated resonant tunneling process dominates the transport (i.e., the electron does not physically dwell on the molecule during transport).[62,63] In these experiments, a clear peak in the conductance near the redox potential of the molecule appears during gating (Figure 7D, E). A maximum in the conductance close to the electrochemical redox potential of the molecule is consistent with the two-step electron transfer process described by Kuznetsov and Ulstrup (KU model).[64,65] Based on this model, the appearance of the maximum in the tunnel/junction current could be rationalized as follows: The

DOI: 10.1021/acs.jpcc.6b06229
J. Phys. Chem. C 2016, 120, 22646−22654

formation of a molecular junction implies that a molecule with discrete electronic levels is located in the gap between substrate and tip. Sweeping the gate potential is equivalent to a parallel shift of the Fermi levels of the tip and substrate. The current first rises as the redox level approaches one of the Fermi levels, and a further increase of the potential leads to a decrease in the current as vacant levels of the positively biased electrode become increasingly thermally inaccessible. This theoretical treatment considers the electron transfer in a redox-molecule functionalized tunnelling junction as two consecutive interfacial single electron transfer steps with vibration relaxation between the steps.[65,66] The process comprises a cycle of consecutive molecular reduction and reoxidation. Because of the position of the observed peak in the conductance versus gate traces, we favor the sequential two-step electron transfer mechanism to explain the experimental results.

4. CONCLUSIONS

Three pyrrolidine-substituted PTCDI molecules have been designed for charge transport study at the single-molecule level. We have investigated the electrochemical and electron transport properties of a series of custom-designed pyrrolidine-substituted PTCDI molecules using cyclic voltammetry and electrochemical STM break junction methods. The substitution of pyrrolidinyl groups at the bay position of PTCDI molecules changed the LUMO/HOMO bandgap of these redox molecules from 2.5 to 2.1 eV. The electrochemical gate effect on molecular conductance was studied by the tapping method as well as by measuring the current vs gate potential when a molecule was bridged between the two working electrodes, named "blinking-and-gating" experiments. The single-molecule conductance of these small-bandgap PTCDI derivatives is about 2−3 times higher than the normal PTCDIs. The cyclic voltammograms of the three studied molecules show the well-defined redox current peaks. This work attempts to explore single-molecule conductance and electrochemical gate effect by tuning the bandgap of a molecular system without significantly altering the conductance pathway. The results indicates that charge transport near the redox potential in these molecular systems is dominated by a two-step charge transport process rather than resonant tunnelling.

■ ASSOCIATED CONTENT

Supporting Information

The Supporting Information is available free of charge on the ACS Publications website at DOI: 10.1021/acs.jpcc.6b06229.

Plotting of current versus bias voltage applied; example current vs distance traces in a control experiment; cyclic voltammograms of molecules 1 and 3 in aqueous solution; UV−vis spectra of three pyrrolidine-substituted perylene tetracarboxylic diimide (PTCDI)

■ AUTHOR INFORMATION

Corresponding Authors

*E-mail: zli6@bsu.edu.
*E-mail: jhihath@ucdavis.edu.
*E-mail: lzang@eng.utah.edu.

Notes

The authors declare no competing financial interest.

■ ACKNOWLEDGMENTS

Z.L. acknowledges Ball State University's ASPiRE program (ASPiRE Junior Faculty Research Awards) for supporting student research; J.H. acknowledges support from the NSF ECCS-1231915; L.Z. thanks the NSF for support (CBET 1502433).

■ REFERENCES

(1) Nitzan, A.; Ratner, M. A. Electron Transport in Molecular Wire Junctions. *Science* **2003**, *300*, 1384−1389.
(2) Cuevas, J. C.; Scheer, E. *Molecular Electronics: An Introduction to Theory and Experiment*; World Scientific Series in Nanotechnology and Nanoscience; World Scientific: Singapore, 2010
(3) Capozzi, B.; Xia, J. L.; Adak, O.; Dell, E. J.; Liu, Z. F.; Taylor, J. C.; Neaton, J. B.; Campos, L. M.; Venkataraman, L. Single-Molecule Diodes with High Rectification Ratios through Environmental Control. *Nat. Nanotechnol.* **2015**, *10*, 522−527.
(4) Donhauser, Z. J.; Mantooth, B. A.; Kelly, K. F.; Bumm, L. A.; Monnell, J. D.; Stapleton, J. J.; Price, D. W.; Rawlett, A. M.; Allara, D. L.; Tour, J. M.; Weiss, P. S. Conductance Switching in Single Molecules through Conformational Changes. *Science* **2001**, *292*, 2303−2307.
(5) Reed, M. A.; Zhou, C.; Muller, C. J.; Burgin, T. P.; Tour, J. M. Conductance of a Molecular Junction. *Science* **1997**, *278*, 252−254.
(6) Lafferentz, L.; Ample, F.; Yu, H.; Hecht, S.; Joachim, C.; Grill, L. Conductance of a Single Conjugated Polymer as a Continuous Function of Its Length. *Science* **2009**, *323*, 1193−1197.
(7) Song, H.; Reed, M. A.; Lee, T. Single Molecule Electronic Devices. *Adv. Mater.* **2011**, *23*, 1583−1608.
(8) Xu, B. Q.; Tao, N. J. Measurement of Single-Molecule Resistance by Repeated Formation of Molecular Junctions. *Science* **2003**, *301*, 1221−1223.
(9) Venkataraman, L.; Klare, J. E.; Nuckolls, C.; Hybertsen, M. S.; Steigerwald, M. L. Dependence of Single-Molecule Junction Conductance on Molecular Conformation. *Nature* **2006**, *442*, 904−907.
(10) Haiss, W.; van Zalinge, H.; Higgins, S. J.; Bethell, D.; Hobenreich, H.; Schiffrin, D. J.; Nichols, R. J. Redox State Dependence of Single Molecule Conductivity. *J. Am. Chem. Soc.* **2003**, *125*, 15294−15295.
(11) Kiguchi, M.; Takahashi, T.; Kanehara, M.; Teranishi, T.; Murakoshi, K. Effect of End Group Position on the Formation of a Single Porphyrin Molecular Junction. *J. Phys. Chem. C* **2009**, *113*, 9014−9017.
(12) Gonzalez, M. T.; Wu, S. M.; Huber, R.; van der Molen, S. J.; Schonenberger, C.; Calame, M. Electrical Conductance of Molecular Junctions by a Robust Statistical Analysis. *Nano Lett.* **2006**, *6*, 2238−2242.
(13) Guedon, C. M.; Valkenier, H.; Markussen, T.; Thygesen, K. S.; Hummelen, J. C.; van der Molen, S. J. Observation of Quantum Interference in Molecular Charge Transport. *Nat. Nanotechnol.* **2012**, *7*, 305−309.
(14) Li, C.; Mishchenko, A.; Li, Z.; Pobelov, I.; Wandlowski, T.; Li, X. Q.; Wurthner, F.; Bagrets, A.; Evers, F. Electrochemical Gate-Controlled Electron Transport of Redox-Active Single Perylene Bisimide Molecular Junctions. *J. Phys.: Condens. Matter* **2008**, *20*, 374122.
(15) Chang, S.; He, J.; Zhang, P. M.; Gyarfas, B.; Lindsay, S. Gap Distance and Interactions in a Molecular Tunnel Junction. *J. Am. Chem. Soc.* **2011**, *133*, 14267−14269.
(16) Dulic, D.; Pump, F.; Campidelli, S.; Lavie, P.; Cuniberti, G.; Filoramo, A. Controlled Stability of Molecular Junctions. *Angew. Chem., Int. Ed.* **2009**, *48*, 8273−8276.
(17) Reichert, J.; Ochs, R.; Beckmann, D.; Weber, H. B.; Mayor, M.; von Lohneysen, H. Driving Current through Single Organic Molecules. *Phys. Rev. Lett.* **2002**, *88*, 176804.

DOI: 10.1021/acs.jpcc.6b06229
J. Phys. Chem. C 2016, 120, 22646−22654

(18) Kumar, A.; Heimbuch, R.; Poelsema, B.; Zandvliet, H. J. W. Controlled Transport through a Single Molecule. *J. Phys.: Condens. Matter* **2012**, *24*, 082201.
(19) Perrin, M. L.; Prins, F.; Martin, C. A.; Shaikh, A. J.; Eelkema, R.; van Esch, J. H.; Briza, T.; Kaplanek, R.; Kral, V.; van Ruitenbeek, J. M.; van der Zant, H. S. J.; Dulic, D. Influence of the Chemical Structure on the Stability and Conductance of Porphyrin Single-Molecule Junctions. *Angew. Chem., Int. Ed.* **2011**, *50*, 11223−11226.
(20) Li, Z. H.; Smeu, M.; Rives, A.; Maraval, V.; Chauvin, R.; Ratner, M. A.; Borguet, E. Towards Graphyne Molecular Electronics. *Nat. Commun.* **2015**, *6*, 6321.
(21) Diez-Perez, I.; Li, Z. H.; Hihath, J.; Li, J. H.; Zhang, C. Y.; Yang, X. M.; Zang, L.; Dai, Y. J.; Feng, X. L.; Muellen, K.; Tao, N. J. Gate-Controlled Electron Transport in Coronenes as a Bottom-up Approach Towards Graphene Transistors. *Nat. Commun.* **2010**, *1*, 1−5.
(22) Sedghi, G.; García-Suárez, V. M.; Esdaile, L. J.; Anderson, H. L.; Lambert, C. J.; Martin, S.; Bethell, D.; Higgins, S. J.; Elliott, M.; Bennett, N.; Macdonald, J. E.; Nichols, R. J. Long-Range Electron Tunnelling in Oligo-Porphyrin Molecular Wires. *Nat. Nanotechnol.* **2011**, *6*, 517−522.
(23) Choi, S. H.; Kim, B.; Frisbie, C. D. Electrical Resistance of Long Conjugated Molecular Wires. *Science* **2008**, *320*, 1482−1486.
(24) Hines, T.; Diez-Perez, I.; Hihath, J.; Liu, H. M.; Wang, Z. S.; Zhao, J. W.; Zhou, G.; Muellen, K.; Tao, N. J. Transition from Tunneling to Hopping in Single Molecular Junctions by Measuring Length and Temperature Dependence. *J. Am. Chem. Soc.* **2010**, *132*, 11658−11664.
(25) Choi, S. H.; Risko, C.; Delgado, M. C. R.; Kim, B.; Bredas, J. L.; Frisbie, C. D. Transition from Tunneling to Hopping Transport in Long, Conjugated Oligo-Imine Wires Connected to Metals. *J. Am. Chem. Soc.* **2010**, *132*, 4358−4368.
(26) Lu, Q.; Liu, K.; Zhang, H. M.; Du, Z. B.; Wang, X. H.; Wang, F. S. From Tunneling to Hopping: A Comprehensive Investigation of Charge Transport Mechanism in Molecular Junctions Based on Oligo(p-Phenylene Ethynylene)S. *ACS Nano* **2009**, *3*, 3861−3868.
(27) Yamada, R.; Kumazawa, H.; Tanaka, S.; Tada, H. Electrical Resistance of Long Oligothiophene Molecules. *Appl. Phys. Express* **2009**, *2*, 025002.
(28) Mishchenko, A.; Zotti, L. A.; Vonlanthen, D.; Burkle, M.; Pauly, F.; Cuevas, J. C.; Mayor, M.; Wandlowski, T. Single-Molecule Junctions Based on Nitrile-Terminated Biphenyls: A Promising New Anchoring Group. *J. Am. Chem. Soc.* **2011**, *133*, 184−187.
(29) Li, Z.; Smeu, M.; Ratner, M. A.; Borguet, E. Effect of Anchoring Groups on Single Molecule Charge Transport through Porphyrins. *J. Phys. Chem. C* **2013**, *117*, 14890−14898.
(30) Lortscher, E.; Cho, C. J.; Mayor, M.; Tschudy, M.; Rettner, C.; Riel, H. Influence of the Anchor Group on Charge Transport through Single-Molecule Junctions. *ChemPhysChem* **2011**, *12*, 1677−1682.
(31) Chen, F.; Li, X. L.; Hihath, J.; Huang, Z. F.; Tao, N. J. Effect of Anchoring Groups on Single-Molecule Conductance: Comparative Study of Thiol-, Amine-, and Carboxylic-Acid-Terminated Molecules. *J. Am. Chem. Soc.* **2006**, *128*, 15874−15881.
(32) Kim, B.; Beebe, J. M.; Jun, Y.; Zhu, X. Y.; Frisbie, C. D. Correlation between Homo Alignment and Contact Resistance in Molecular Junctions: Aromatic Thiols Versus Aromatic Isocyanides. *J. Am. Chem. Soc.* **2006**, *128*, 4970−4971.
(33) Zotti, L. A.; Kirchner, T.; Cuevas, J. C.; Pauly, F.; Huhn, T.; Scheer, E.; Erbe, A. Revealing the Role of Anchoring Groups in the Electrical Conduction through Single-Molecule Junctions. *Small* **2010**, *6*, 1529−1535.
(34) Martin, C. A.; Ding, D.; Sorensen, J. K.; Bjornholm, T.; van Ruitenbeek, J. M.; van der Zant, H. S. J. Fullerene-Based Anchoring Groups for Molecular Electronics. *J. Am. Chem. Soc.* **2008**, *130*, 13198−13199.
(35) Arroyo, C. R.; Leary, E.; Castellanos-Gomez, A.; Rubio-Bollinger, G.; Gonzalez, M. T.; Agrait, N. Influence of Binding Groups on Molecular Junction Formation. *J. Am. Chem. Soc.* **2011**, *133*, 14313−14319.
(36) Schneebeli, S. T.; Kamenetska, M.; Cheng, Z. L.; Skouta, R.; Friesner, R. A.; Venkataraman, L.; Breslow, R. Single-Molecule Conductance through Multiple Pi−Pi-Stacked Benzene Rings Determined with Direct Electrode-to-Benzene Ring Connections. *J. Am. Chem. Soc.* **2011**, *133*, 2136−2139.
(37) Xiao, X. Y.; Xu, B. Q.; Tao, N. J. Conductance Titration of Single-Peptide Molecules. *J. Am. Chem. Soc.* **2004**, *126*, 5370−5371.
(38) Li, Z.; Smeu, M.; Afsari, S.; Xing, Y. J.; Ratner, M. A.; Borguet, E. Single-Molecule Sensing of Environmental Ph-an STM Break Junction and NEGF-DFT Approach. *Angew. Chem., Int. Ed.* **2014**, *53*, 1098−1102.
(39) Xu, B. Q.; Xiao, X. Y.; Tao, N. J. Measurements of Single-Molecule Electromechanical Properties. *J. Am. Chem. Soc.* **2003**, *125*, 16164−16165.
(40) Guo, S. Y.; Artes, J. M.; Diez-Perez, I. Electrochemically-Gated Single-Molecule Electrical Devices. *Electrochim. Acta* **2013**, *110*, 741−753.
(41) Li, Z. H.; Li, H.; Chen, S. J.; Froehlich, T.; Yi, C. Y.; Schonenberger, C.; Calame, M.; Decurtins, S.; Liu, S. X.; Borguet, E. Regulating a Benzodifuran Single Molecule Redox Switch via Electrochemical Gating and Optimization of Molecule/Electrode Coupling. *J. Am. Chem. Soc.* **2014**, *136*, 8867−8870.
(42) Kay, N. J.; Higgins, S. J.; Jeppesen, J. O.; Leary, E.; Lycoops, J.; Ulstrup, J.; Nichols, R. J. Single-Molecule Electrochemical Gating in Ionic Liquids. *J. Am. Chem. Soc.* **2012**, *134*, 16817−16826.
(43) Li, Y.; Kaneko, S.; Fujii, S.; Kiguchi, M. Symmetry of Single Hydrogen Molecular Junction with Au, Ag, and Cu Electrodes. *J. Phys. Chem. C* **2015**, *119*, 19143−19148.
(44) Ko, C. H.; Huang, M. J.; Fu, M. D.; Chen, C. H. Superior Contact for Single-Molecule Conductance: Electronic Coupling of Thiolate and Isothiocyanate on Pt, Pd, and Au. *J. Am. Chem. Soc.* **2010**, *132*, 756−764.
(45) Ballmann, S.; Hartle, R.; Coto, P. B.; Elbing, M.; Mayor, M.; Bryce, M. R.; Thoss, M.; Weber, H. B. Experimental Evidence for Quantum Interference and Vibrationally Induced Decoherence in Single-Molecule Junctions. *Phys. Rev. Lett.* **2012**, *109*, 056801.
(46) Tuxen, J.; Gerlich, S.; Eibenberger, S.; Arndt, M.; Mayor, M. Quantum Interference Distinguishes between Constitutional Isomers. *Chem. Commun.* **2010**, *46*, 4145−4147.
(47) Kim, Y.; Song, H.; Strigl, F.; Pernau, H. F.; Lee, T.; Scheer, E. Conductance and Vibrational States of Single-Molecule Junctions Controlled by Mechanical Stretching and Material Variation. *Phys. Rev. Lett.* **2011**, *106*, 196804.
(48) Quek, S. Y.; Kamenetska, M.; Steigerwald, M. L.; Choi, H. J.; Louie, S. G.; Hybertsen, M. S.; Neaton, J. B.; Venkataraman, L. Mechanically Controlled Binary Conductance Switching of a Single-Molecule Junction. *Nat. Nanotechnol.* **2009**, *4*, 230−234.
(49) Katsonis, N.; Kudernac, T.; Walko, M.; van der Molen, S. J.; van Wees, B. J.; Feringa, B. L. Reversible Conductance Switching of Single Diarylethenes on a Gold Surface. *Adv. Mater.* **2006**, *18*, 1397−1400.
(50) Lara-Avila, S.; Danilov, A. V.; Kubatkin, S. E.; Broman, S. L.; Parker, C. R.; Nielsen, M. B. Light-Triggered Conductance Switching in Single-Molecule Dihydroazulene/Vinylheptafulvene Junctions. *J. Phys. Chem. C* **2011**, *115*, 18372−18377.
(51) Tam, E. S.; Parks, J. J.; Shum, W. W.; Zhong, Y. W.; Santiago-Berrios, M. B.; Zheng, X.; Yang, W. T.; Chan, G. K. L.; Abruna, H. D.; Ralph, D. C. Single-Molecule Conductance of Pyridine-Terminated Dithienylethene Switch Molecules. *ACS Nano* **2011**, *5*, 5115−5123.
(52) Diez-Perez, I.; Li, Z. H.; Guo, S. Y.; Madden, C.; Huang, H. L.; Che, Y. K.; Yang, X. M.; Zang, L.; Tao, N. J. Ambipolar Transport in an Electrochemically Gated Single-Molecule Field-Effect Transistor. *ACS Nano* **2012**, *6*, 7044−7052.
(53) Xu, B. Q.; Xiao, X. Y.; Yang, X. M.; Zang, L.; Tao, N. J. Large Gate Modulation in the Current of a Room Temperature Single Molecule Transistor. *J. Am. Chem. Soc.* **2005**, *127*, 2386−2387.
(54) Frisenda, R.; Parlato, L.; Barra, M.; van der Zant, H. S. J.; Cassinese, A. Single-Molecule Break Junctions Based on a Perylene-Diimide Cyano-Functionalized (PDI8-CN2) Derivative. *Nanoscale Res. Lett.* **2015**, *10* (305), 1−7.

DOI: 10.1021/acs.jpcc.6b06229
J. Phys. Chem. C 2016, 120, 22646−22654

(55) Li, C.; Stepanenko, V.; Lin, M. J.; Hong, W. J.; Wurthner, F.; Wandlowski, T. Charge Transport through Perylene Bisimide Molecular Junctions: An Electrochemical Approach. *Phys. Status Solidi B-Basic Solid State Phys.* **2013**, *250*, 2458−2467.
(56) White, H. S.; Kittlesen, G. P.; Wrighton, M. S. Chemical Derivatization of an Array of 3 Gold Microelectrodes with Polypyrrole—Fabrication of a Molecule-Based Transistor. *J. Am. Chem. Soc.* **1984**, *106*, 5375−5377.
(57) Chen, F.; He, J.; Nuckolls, C.; Roberts, T.; Klare, J. E.; Lindsay, S. A Molecular Switch Based on Potential-Induced Changes of Oxidation State. *Nano Lett.* **2005**, *5*, 503−506.
(58) Li, Z.; Han, B.; Meszaros, G.; Pobelov, I.; Wandlowski, T.; Blaszczyk, A.; Mayor, M. Two-Dimensional Assembly and Local Redox-Activity of Molecular Hybrid Structures in an Electrochemical Environment. *Faraday Discuss.* **2006**, *131*, 121−143.
(59) Capozzi, B.; Chen, Q. S.; Darancet, P.; Kotiuga, M.; Buzzeo, M.; Neaton, J. B.; Nuckolls, C.; Venkataraman, L. Tunable Charge Transport in Single-Molecule Junctions via Electrolytic Gating. *Nano Lett.* **2014**, *14*, 1400−1404.
(60) Aguilar-Sanchez, R.; Su, G. J.; Homberger, M.; Simon, U.; Wandlowski, T. H. Structure and Electrochemical Characterization of 4-Methyl-4′-(*N*-mercaptoalkyl)biphenyls on Au(111)-(1 × 1). *J. Phys. Chem. C* **2007**, *111*, 17409−17419.
(61) Li, X. L.; Hihath, J.; Chen, F.; Masuda, T.; Zang, L.; Tao, N. J. Thermally Activated Electron Transport in Single Redox Molecules. *J. Am. Chem. Soc.* **2007**, *129*, 11535−11542.
(62) Schmickler, W.; Widrig, C. The Investigation of Redox Reactions with a Scanning Tunneling Microscope—Experimental and Theoretical Aspects. *J. Electroanal. Chem.* **1992**, *336*, 213−221.
(63) Schmickler, W. Tunneling of Electrons through Thin-Layers of Water. *Surf. Sci.* **1995**, *335*, 416−421.
(64) Zhang, J.; Chi, Q.; Kuznetsov, A. M.; Hansen, A. G.; Wackerbarth, H.; Christensen, H. E. M.; Andersen, J. E. T.; Ulstrup, J. Electronic Properties of Functional Biomolecules at Metal/Aqueous Solution Interfaces. *J. Phys. Chem. B* **2002**, *106*, 1131−1152.
(65) Kuznetsov, A. M.; Ulstrup, J. Mechanisms of in Situ Scanning Tunnelling Microscopy of Organized Redox Molecular Assemblies. *J. Phys. Chem. A* **2000**, *104*, 11531−11540.
(66) Li, Z. H.; Liu, Y. Q.; Mertens, S. F. L.; Pobelov, I. V.; Wandlowski, T. From Redox Gating to Quantized Charging. *J. Am. Chem. Soc.* **2010**, *132*, 8187−8193.

DOI: 10.1021/acs.jpcc.6b06229
J. Phys. Chem. C 2016, 120, 22646−22654